Opto-VLSI-based reconfigurable Photonic RF Filter

Feng Xiao*, Mingya Shen, Budi Juswardy, and Kamal Alameh

Centre of Excellence for MicroPhotonic System, Edith Cowan University
270 Joondalup Drive, Joondalup WA 6027 Australia.

ABSTRACT

Radio frequency (RF) signal processors based on photonics have several advantages, such as broadband capability, immunity to electromagnetic interference, flexibility, and light weight in comparison to all-electronics RF filters. It still requires innovative research and development to achieve high-resolution reconfigurable photonic RF signal processors featuring high selectivity, resolution, wide tunability, and fast reconfigurability. In this paper, we propose and experimentally demonstrate the concept of a reconfigurable photonic RF filter structure integrating an Amplified Spontaneous Emission (ASE) source, an Opto-VLSI processor that generates arbitrary phase-only steering and multicasting holograms for wavelength selection and attenuation, arrayed waveguide gratings (AWGs) for waveband multiplexing and demultiplexing, high-dispersion fibres for RF delay synthesis, and a balanced photodetector for generating positive and negative processor weights. Independent control of the weights of a reconfigurable photonic RF filter is experimentally demonstrated.

Keywords: Opto-VLSI, Photonic Filter, MicroPhotonic, Microwave photonics.

1. INTRODUCTION

Photonic-based radio frequency (RF) filters have many advantages including immunity to electromagnetic interference (EMI), flexibility, broadband capability and light weight compared to RF filter implemented using electronic circuits. These advantages open new opportunities in a wide range of potential applications where high selectivity, resolution, wide tunability, and fast reconfigurability characteristics are required [1].

Several tunable photonic RF filter structures have been proposed and demonstrated [1-6]. In these demonstrations, filter reconfigurability is achieved by adjusting the tap weights through optical attenuation via MEMS switches [2], using variable optical attenuators (VOAs) [4], or employing Fiber Bragg Gratings (FBG) [5] that can be tuned either thermally or mechanically. However, in order to achieve high-resolution reconfigurable photonic RF signal processors that are able to synthesise arbitrary transfer characteristics, extensive research and development are still needed [6].

In this paper, a reconfigurable photonic RF filter structure employing a broadband optical source, a pair of Arrayed Waveguide Gratings (AWG), an Opto-VLSI processor, a pair of high-dispersion fibres, and a balanced photodetector is proposed to synthesize arbitrary RF responses through optical beam steering and multicasting as well as optical true-time delay generation.

2. OPTO-VLSI PROCESSOR

A reconfigurable Opto-VLSI processor comprises an array of liquid crystal (LC) cells driven by a Very-Large-Scale-Integrated (VLSI) circuit that generates digital holographic diffraction gratings to steer and/or shape optical beams [7,8], as illustrated in Fig. 1. Each pixel is assigned a few memory elements that store a digital value, and a multiplexer that selects one of the input voltages and applies it to the aluminium mirror plate. Opto-VLSI processors are electronically controlled, software-configured, polarization independent, cost effective, and very reliable since beam steering is achieved with no mechanically moving parts. Fig. 1 also shows a typical layout and a cell design of an 8-phase Opto-VLSI processor. By applying programmed control signal on the electrodes, the liquid crystal behaves like a phase grating with both its phase amplitudes and the grating spatial distribution digitalized to simulate a linear phase grating, as illustrated in Fig. 2. When an optical beam illuminates a 2-D Opto-VLSI processor with a small incident angle, the x-direction θ_x or y-direction θ_y of the 1st-order diffractive beam is determined by grating equation [7-8]:

$$\theta_{x/y} \approx \lambda/p_{x/y} = \lambda/(S_{x/y}*N_{x/y}) \quad (1)$$

* Further author information:
E-mail: f.xiao@ecu.edu.au, Telephone: 61 8 6304 5732

Photonics and Optoelectronics Meetings (POEM) 2009: Optoelectronic Devices and Integration, edited by Zishen Zhao, Ray Chen, Yong Chen, Jinzhong Yu, Junqiang Sun, Proc. of SPIE Vol. 7516, 75160H · © 2009 SPIE · CCC code: 0277-786X/09/$18 · doi: 10.1117/12.843432

where p is grating period, S is the size of rectangular liquid crystal pixels and N is the number of the pixels in a period of the grating. The digitalized phase levels can be expressed as:

$$\varphi_i = i*(2\pi/M),\ i=1,2,\ldots,M \tag{2}$$

where M is the number of discrete phase levels, and the phases of the pixels in a period have discrete values from $2\pi/M$ to 2π.

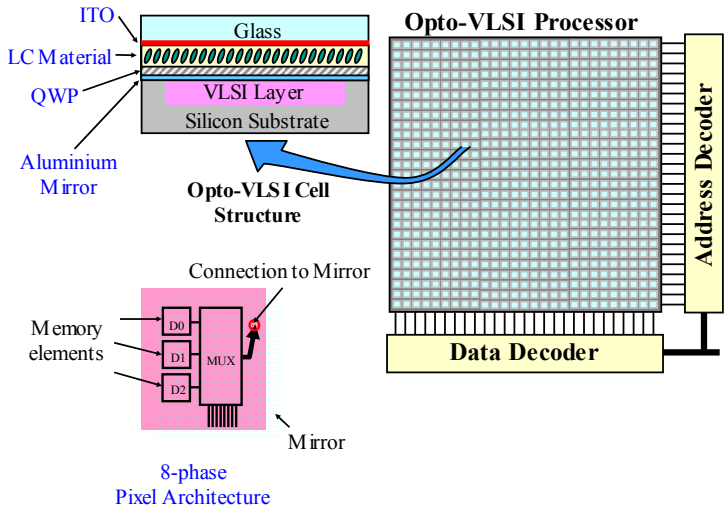

Fig. 1. Typical 8-phase Opto-VLSI processor and LC cell structure

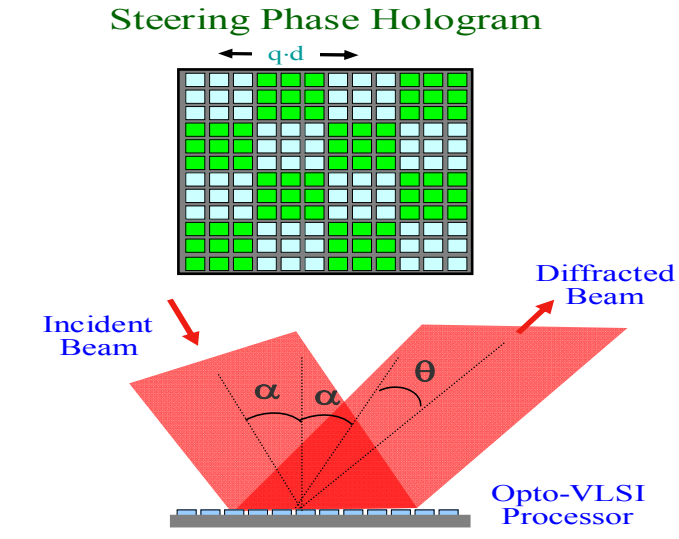

Fig. 2. Steering capability of an Opto-VLSI processor.

3. MICROWAVE PHOTONIC FILTER STRUCTURE

The structure of the photonic RF filters shown in Fig. 3. A broadband light source of amplified spontaneous emission

(ASE) is externally modulated by the RF signal through an electro-optic modulator (EOM). The modulated light is routed via a circulator into an N-channel arrayed waveguide grating (AWG 1) that slices the ASE into different RF-modulated wavebands, which are routed to a fiber array of N fiber pairs. Each fiber pair consists of an upper fiber (connected to an output port of AWG 1) and a lower fiber (connected to a corresponding port of AWG 2). The lower fiber is parallel to the upper fiber with a space of 0.25μm, and the spacing between adjacent fiber pairs is 1 mm. A lens array with a pitch of 1 mm is used to convert the divergent beams from the upper optical fibers into collimated beams.

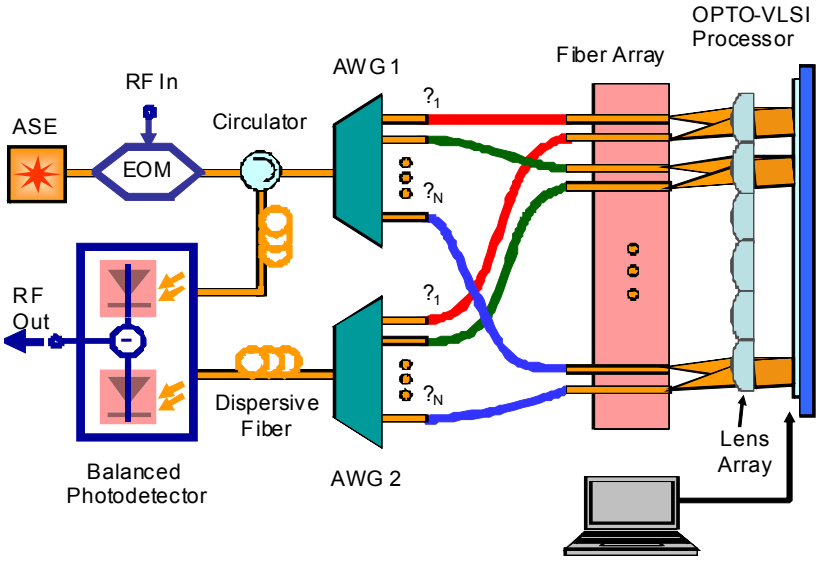

Fig. 3. Proposed reconfigurable photonic RF filter based on an Opto-VLSI processor and a 4f imaging system.

By employing an appropriate hologram into the Opto-VLSI processor, the collimated beam is appropriately steered and coupled with arbitrary attenuation (or weight) to either the upper fiber (for positive weights) or to the lower fiber port (for negative weights). The wavelengths from the lower ports are multiplexed via AWG 2 and delayed by a high dispersion fiber, while the remaining wavelengths, which are steered and coupled back into the upper fibers, are multiplexed by AWG 1 and reach another similar high dispersion fiber via the circulator. The two multiplexed WDM signals are detected by a pair of balanced photodiodes which generate delayed versions of the input RF signal with positive and negative weights that are controlled by the phase holograms uploaded onto the Opto-VLSI processor, thus realizing an arbitrary transfer function.

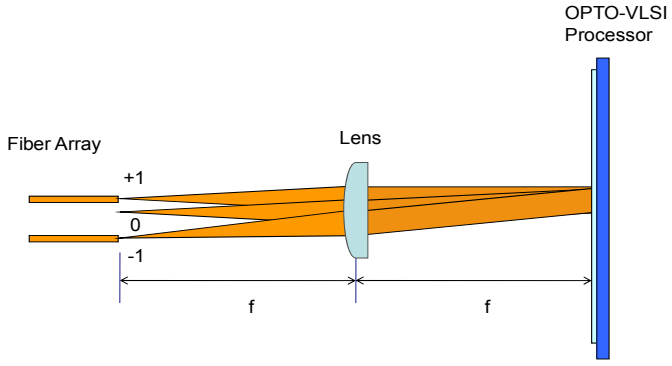

Fig. 4. 4f imaging system. The beam can be steered to the upper fiber port and the lower fiber port by the hologram uploaded onto the Opto-VLSI processor.

Note that the distance between the lens array and the fiber array is f, the focal length of each lens, equal to that between the lens array and the Opto-VLSI processor, as shown in Fig. 4. When no hologram is applied, the input beam from the upper fiber is collimated by the lens, reflected back, and focused again by the same lens. The position of this

focused beam (so called 0^{th} order), which can be adjusted by shifting the fiber array up and down according to the lens array, locates between the fiber pair. By uploading a phase hologram onto the Opto-VLSI processor, the incident collimated optical beam can be diffracted so that the $+1^{th}$ diffraction order can be coupled into the upper fiber as positive coefficient signal or -1^{th} order diffraction into the lower fiber as negative coefficient signal, as showed in Fig. 4. This technique eliminates the need for customized tilt arrayed fibers, leading to simple and low-cost tunable microwave filter systems.

4. SIMULATED RESULTS

The response of the photonic RF signal processor shown in Fig. 3 can be expressed as

$$H(\omega) = \sum_{k=0}^{N-1} a_k e^{-j\cdot\omega\cdot k\cdot T} - \sum_{k=0}^{N-1} b_k e^{-j\cdot\omega\cdot k\cdot T} \tag{3}$$

where N is the number of the taps, a_k is the weight associated with the optical intensity of the k^{th} waveband centered at λ_k, coupled into the k^{th} upper optical fibre and detected by the upper photodetector; b_k is the weight associated with the optical intensity of the k^{th} waveband centered at λ_k, coupled into the k^{th} lower optical fiber and detected by the lower photodetector.

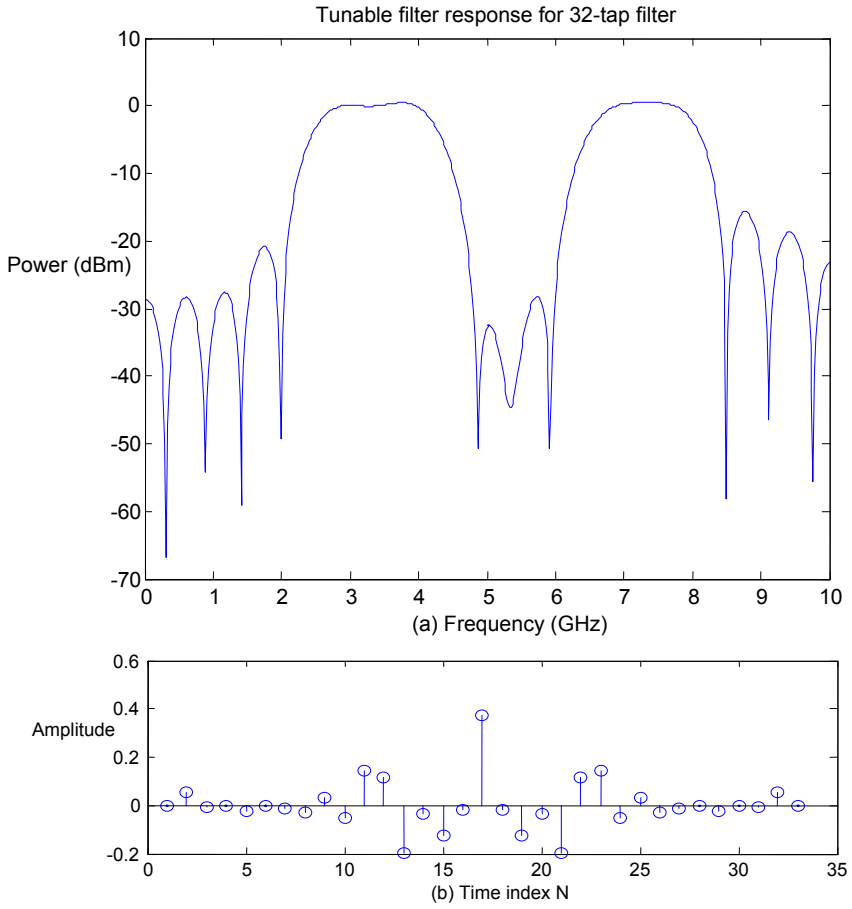

Fig. 5. Examples of filter responses and weights used to synthesize passbands at 3.5 GHz and 7.2 GHz. (a) 32-waveband filter response, and (b) 32 waveband weights.

A computer algorithm has been developed to optimize the tap weights, a_k and b_k that synthesize a specific filter

response and are used to generate the appropriate phase holograms to be uploaded onto the Opto-VLSI processor. Fig 5(a) shows simulated 32-waveband dual passband filter response, where only steering holograms are used to generate the filter's 32 weights. Fig 5(b) shows the weights of the corresponding 32 wavebands. Note that, a much improved filter shape factor is seen when multicasting is employed.

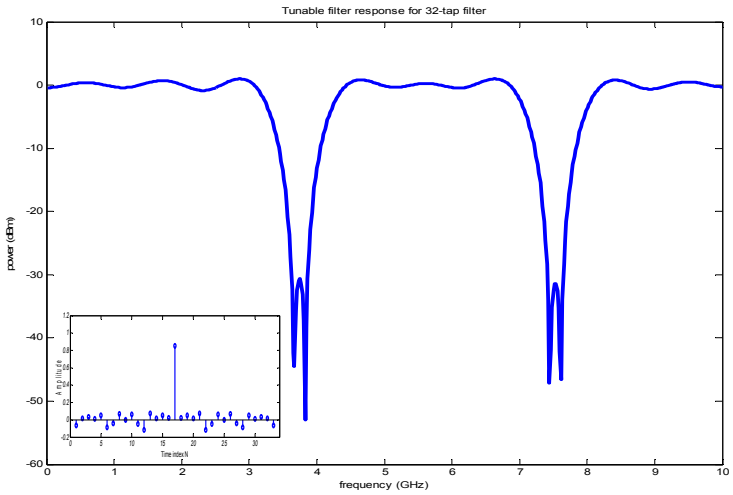

Fig. 6. Notch-filter response and weights (inset) of a 32-tap filter structure with notch frequencies at 3.75 GHz and at 7.5 GHz.

Fig. 6 show examples of notch filter responses and their corresponding weights where the notch frequencies are selected at 3.75 GHz to 7.5 GHz.

5. EXPERIMENTAL RESULTS AND DISCUSSION

The experimental setup to proof the principle is shown in Fig. 7. The Opto-VLSI processor is 1-D liquid crystal on silicon with 4096 pixels, each of which has 1 μm pixel size and 0.8 μm dead spacing between adjacent pixels. Two wavelength channels λ_1=1547.5nm and λ_2=1530.3nm coming from two tunable laser sources were sent to a SM-fiber array via two optical circulators; one signal was routed to fiber 1 and the other to fiber 7. The optical beams diverging from fiber 1 and fiber 7 were collimated by a 4-lens array. Each lens is AR coated with reflection rate R<0.5%, and has diameter of 950 μm and focal length of 2420 μm. The collimated beams illuminate the surface of the Opto-VLSI processor where two optimized phase holograms were applied to steer these two beams with appropriate attenuation either back to their corresponding fiber ports for positive weights or respectively couple them to fiber 2 and fiber 8 for negative weights. Two optical spectrum analyzers (OSAs) were used to monitor the signals.

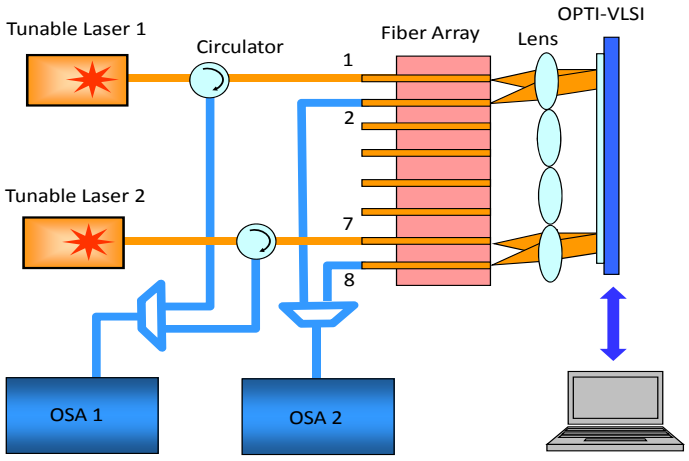

Fig. 7. Experimental setup to demonstrate the concept of the photonic RF signal processor.

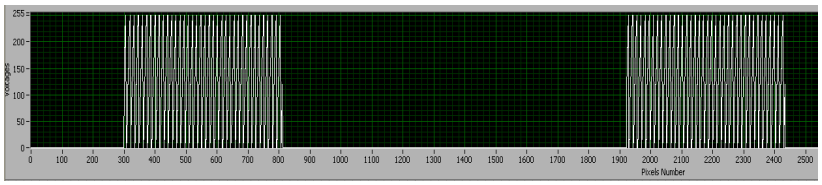

Fig. 8. Two phase gratings were generated to control positive and negative weights.

Two phase holograms were generated to control positive and negative weights. The first hologram was used to steer λ_1 form fiber port 1 to fiber port 1 for positive detection and the second steered λ_2 from fiber port 7 to fiber port 8 for negative detection, as shown in Fig. 8. Each of the two gratings had approximate 500 pixels and was optimized for maximal coupling efficiency to desired fiber ports and minimum crosstalk to undesired fiber ports. A LabVIEW program was designed to generate and optimize the phase holograms for all the operations.

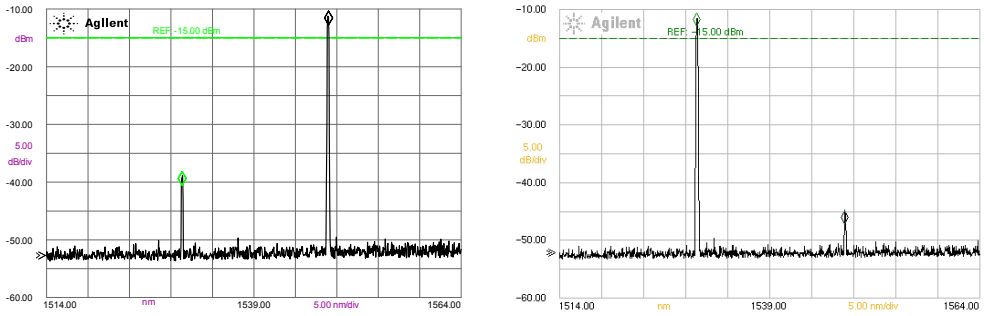

(a) (b)

Fig.9. Experimental results showing the incident signals can be controlled for positive and negative weights. (a) The signal with wavelength λ_1 was steered for positive detection; (b) the signal with wavelength λ_2 was steered for negative detection.

Experimental results to demonstrate the selection for positive or negative signal detection are shown in Fig. 9, where the crosstalk is also shown. The signal λ_1 was steered to fiber 1 for positive coefficient and λ_2 was steered to fiber 8 for negative coefficient. The intensities of both signals can be precisely controlled by using different phase holograms. Fig. 10 shows the experimental results for the control of signal attenuation of λ_1. By changing the phase slope of holograms (defined by the ratio of maximum applied voltages to phase periods), the intensity of signal λ_1 can be controlled from -11.9 dBm to -45.2 dBm.

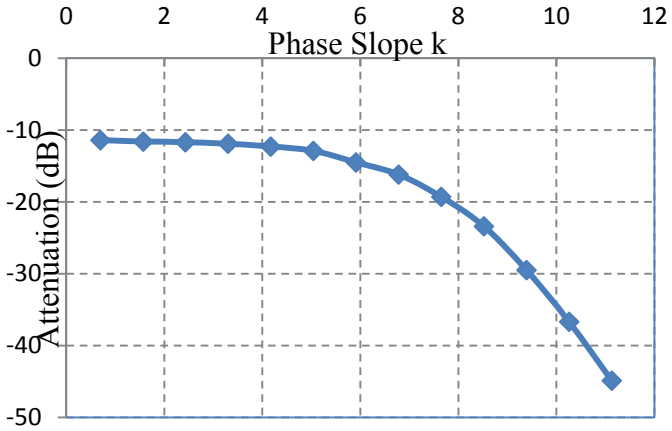

Fig. 10. Attenuation versus phase slope of holograms uploaded onto the Opto-VLSI processor

In these experiments, we are using a 1 x 4096 Opto-VLSI processor to realize 4-tap tunable photonic RF filter. It is important to note that by employing a two-dimensional, 16mm×16mm Opto-VLSI processor, a 256-tap RF filter can practically be realised using 128-channel AWGs.

6. CONCLUSION

A reconfigurable photonic RF filter has been proposed and its principle has been demonstrated. Simulation and experimental results show that arbitrary tap weights can be generated using optimised steering phase holograms uploaded onto the Opto-VLSI processor. We have demonstrated the capability of the proposed structure to generate positive and negative taps, with variable amplitude control.

REFERENCES

1. J. Capmany, B. Ortega, and D. Pastor, "A tutorial on microwave photonic filters," J. Lightw. Technol., 24 (1), 201–229 (2006).
2. J. Capmany, J. Mora, B. Ortega, and D. Pastor, "Microwave photonic filters using low-cost sources featuring tunability, reconfigurability and negative coefficients," Opt. Express, 13 (2), 1412–1417 (2005).
3. V. Polo, B. Vidal, J. L. Corral, and J. Marti, "Novel tunable photonic microwave filter based on laser arrays and N×N AWG-based delay lines," IEEE Photon. Technol. Lett., 15(4), 584–586 (2003).
4. D. Pastor, B. Ortega, J. Capmany, S. Sales, A. Martinez, and P. Muñoz, "Optical microwave filter based on spectral slicing by use of arrayed waveguide gratings," Opt. Lett., 28, 1802-1804 (2003).
5. J. D. Taylor, L. R. Chen, and X. Gu, "Simple reconfigurable photonic microwave filter using an array waveguide grating and fiber Bragg gratings," IEEE Photonics Technology Letters, 19, 510-512 (2007).
6. J. Capmany, B. Ortega, D. Pastor, and S. Sales, "Discrete-time optical processing of microwave signals," Journal of Light Technology, 23, 702-722 (2005).
7. X. H. Wang et al., "Liquid Crystal on Silicon (LCOS) Wavefront Corrector and Beam Steerer", SPIE Proc. 5162, 139-146 (2003).
8. P. McManamon et al., "Optical Phased Array", IEEE Proc. 84 (2), 268-298 (1996).